Cell Research (2015) 25:691-706.
© 2015 IBCB, SIBS, CAS All rights reserved 1001-0602/15 $ 32.00
www.nature.com/cr

ORIGINAL ARTICLE

Park7 interacts with p47^{phox} to direct NADPH oxidase-dependent ROS production and protect against sepsis

Wenjun Liu[1, *], Hailong Wu[1, *], Lili Chen[1], Yankai Wen[1], Xiaoni Kong[1], Wei-Qiang Gao[1]

[1]*State Key Laboratory for Oncogenes and Related Genes, Renji-Med X Clinical Stem Cell Research Center, Ren Ji Hospital, School of Biomedical Engineering, Shanghai Jiao Tong University, Shanghai 200030, China*

Inappropriate inflammation responses contribute to mortality during sepsis. Through Toll-like receptors (TLRs), reactive oxygen species (ROS) produced by NADPH oxidase could modulate the inflammation responses. Parkinson disease (autosomal recessive, early onset) 7 (Park7) has a cytoprotective role by eliminating ROS. However, whether Park7 could modulate inflammation responses and mortality in sepsis is unclear. Here, we show that, compared with wild-type mice, *Park7*$^{-/-}$ mice had significantly increased mortality and bacterial burdens in sepsis model along with markedly decreased systemic and local inflammation, and drastically impaired macrophage phagocytosis and bacterial killing abilities. Surprisingly, LPS and phorbol-12-myristate-13-acetate stimulation failed to induce ROS and proinflammatory cytokine production in *Park7*$^{-/-}$ macrophages and *Park7*-deficient RAW264.7 cells. Through its C-terminus, Park7 binds to p47^{phox}, a subunit of the NADPH oxidase, to promote NADPH oxidase-dependent production of ROS. Restoration of Park7 expression rescues ROS production and improves survival in LPS-induced sepsis. Together, our study shows that Park7 has a protective role against sepsis by controlling macrophage activation, NADPH oxidase activation and inflammation responses.

Keywords**:** *Park7*; inflammation; sepsis; NADPH oxidase

Cell Research (2015) **25**:691-706. doi: 10.1038/cr.2015.63; published online 29 May 2015

Introduction

Sepsis, characterized by a system-wide dysregulation of inflammation responses following primary bacterial infection, is one of the leading causes of death in intensive care unit worldwide [1]. Extravagant inflammation reactions are autodestructive and result in distant organ damage or failure, whereas an insufficient response due to immune anergy or tolerance can propagate further infection [2]. Some septic patients die at the early stage of sepsis characterized by an uncontrolled activation of the immune responses [3], but most patients die at the late stage with significant immunosuppression, marked by an impaired activation of the immune responses and hypoinflammation [4-6]. Therefore, understanding the immune pathophysiology of the late stage will be mandatory for discovering novel therapeutic options.

Reactive oxygen species (ROS) play essential roles in regulating immune responses against pathogens, and are critical to macrophages' bactericidal activity [7, 8]. In addition, ROS could function as signaling molecules to activate multiple signal transduction cascades and in turn modulate inflammatory responses [9-12]. Thus, mediators regulating oxidative stress may effectively modulate inflammation responses and improve survival in sepsis.

Parkinson disease 7 (Park7), also known as DJ-1, is highly conserved in all organisms and has diverse biochemical and cellular activities. Loss-of-function mutations of *PARK7* are considered as causal factors for the early onset of Parkinson's disease (PD). In addition, decreased Park7 levels were detected in cerebrospinal fluid of late-onset PD patients (age > 50) compared with health controls [13]. Oxidative stress has been implicated in the pathogenesis of PD, because neuronal cells with either *Park7* deletion or *Park7* downregulation are sensitive to oxidative stress [14, 15]. Given the antioxidant

*These two authors contributed equally to this work.
Correspondence: Xiaoni Kong[a], Wei-Qiang Gao[b]
[a]Tel: 86-21-34206284
E-mail: xiaonikong@sjtu.edu.cn or xiaonikong@gmail.com
[b]Tel: 86-21-68383917
E-mail: gao.weiqiang@sjtu.edu.cn
Received 23 November 2014; revised 24 March 2015; accepted 7 April 2015; published online 29 May 2015

feature of Park7 and that oxidative stress is tightly related to inflammatory responses and survival in experimental sepsis [12, 16], we hypothesized that Park7 protects against sepsis by modulating the cellular redox state.

In this study, we demonstrate that *Park7* depletion leads to higher susceptibility to sepsis. *Park7*$^{-/-}$ mice present increased bacterial burdens, reduced local and systemic inflammation, macrophage paralysis and impaired induction of proinflammatory cytokines under the condition of sepsis. These immunosuppression phenomena are largely attributable to the inactivation of NADPH oxidase caused by Park7 deficiency. Through its C-terminus, Park7 interacts with p47^{phox} to facilitate NADPH oxidase-dependent ROS production. More importantly, we demonstrate that *in vivo* administration of Park7-restored macrophages rescues animals from septic death induced by LPS. Our findings for the first time demonstrate that Park7 could direct NADPH oxidase activation and indicate the putative therapeutic potential of Park7 in sepsis.

Results

Disruption of Park7 significantly increases lethality but drastically decreases local inflammation during CLP- and LPS-induced sepsis

The absence of Park7 was confirmed in *Park7*$^{-/-}$ mice (Supplementary information, Figure S1A). We first examined the role of Park7 in survival in a septic model induced by cecal ligation and puncture (CLP). 60 h after CLP, 85% of *Park7*$^{-/-}$ mice died while only 40% of WT mice died. After 5 days, 25% of WT mice still survived, whereas 15% of *Park7*$^{-/-}$ mice were alive (Figure 1A). Meanwhile, the higher susceptibility of *Park7*$^{-/-}$ mice was also verified in another clinically relevant septic model induced by *Pseudomonas aeruginosa* infection (Supplementary information, Figure S1B). We then investigated the role of Park7 in survival in LPS-induced sepsis. WT and *Park7*$^{-/-}$ mice were treated i.p. with a lethal dose of LPS (15 mg/kg BW) and survival was monitored for 5 days. 100% of *Park7*$^{-/-}$ mice died within 84 h whereas 30% of WT mice survived by day 5 (Figure 1B). As Park7 is critical for septic survival, the role of Park7 in regulating inflammation was investigated in nonlethal septic models. Lung injury was assessed by histopathology analysis and lung wet/dry ratio 24 h after CLP or LPS treatment (i.p. 5 mg/kg BW). Lung injuries were greatly decreased as indicated by less infiltration of inflammatory cells and lower wet/dry ratio in *Park7*$^{-/-}$ mice compared with WT ones (Figure 1C and 1D). Consistent with these results, much fewer inflammatory cells were observed in bronchoalveolar lavage (BAL) fluid of *Park7*$^{-/-}$ mice compared with WT mice (Figure 1E and 1F). Meanwhile, upon CLP and LPS treatment, significantly reduced recruitment of macrophages to peritoneal cavity was observed in *Park7*$^{-/-}$ mice compared with WT mice (Figure 1G and 1H). In response to impaired recruitment of inflammatory cells, significantly decreased levels of CXCL1, CXCL2 and CCL2 were detected in both peritoneal fluid and BAL fluid in *Park7*$^{-/-}$ mice compared with WT mice after CLP or LPS (Figure 1I-1K and Supplementary information, Figure S1C-S1E). Taken together, these results show that *Park7*$^{-/-}$ mice have greater susceptibility but reduced inflammatory responses to sepsis induced either by endotoxin or by polymicrobial infections.

Park7$^{-/-}$ *mice had greatly reduced secretion of IL-6 and TNF-α after CLP and LPS treatment*

As IL-6 and TNF-α are proinflammatory cytokines elevated during the early septic hyperinflammation and are negatively correlated with the septic survival [17, 18], their concentrations in serum and peritoneal fluid were measured by ELISA. 24 h after CLP or LPS, levels of IL-6 and TNF-α in serum or peritoneal fluid were significantly lower in *Park7*$^{-/-}$mice compared with WT mice (Figure 2A-2D). Furthermore, IL-6 concentrations in BAL fluid were lower in *Park7*$^{-/-}$mice compared with WT mice (Figure 2E and 2F). Given that macrophages are the prime source of inflammatory cytokines [19], levels of IL-6 and TNF-α in peritoneal macrophages were examined by qPCR and ELISA. LPS induced fewer transcripts and less secretion of IL-6 and TNF-α in *Park7*$^{-/-}$ macrophages compared with WT ones (Figure 2G and 2H). Because the secretion of TNF-α usually declines in 24 h, we did not observe significant difference in TNF-α levels 24 h after LPS. Given that IL-10 is a negative regulator of IL-6 and TNF-α upon inflammatory stimulation [20], we then examined whether *Park7*$^{-/-}$ mice has increased IL-10. Interestingly, IL-10 levels in serum and peritoneal fluid were also significantly decreased in *Park7*$^{-/-}$ mice compared with WT mice after CLP or LPS treatment (Figure 2I and 2J). Similarly, less IL-10 induction was detected in *Park7*$^{-/-}$ macrophages after LPS (Figure 2K). We further examined whether Park7 deficiency could affect the IL-6 and TNF-α levels in RAW264.7, a macrophage cell line. Stable transfectants with expression of a *Park7*-shRNA or a shRNA not targeting any genes from mouse were established. *Park7* knockdown was confirmed by qPCR and immunoblotting (Supplementary information, Figure S2A). We refer to NT and KD hereafter as non-target and knockdown groups, respectively. LPS induced significantly fewer IL-6 and TNF-α in KD compared with NT (Supplementary information, Figure S2B-S2E). These results

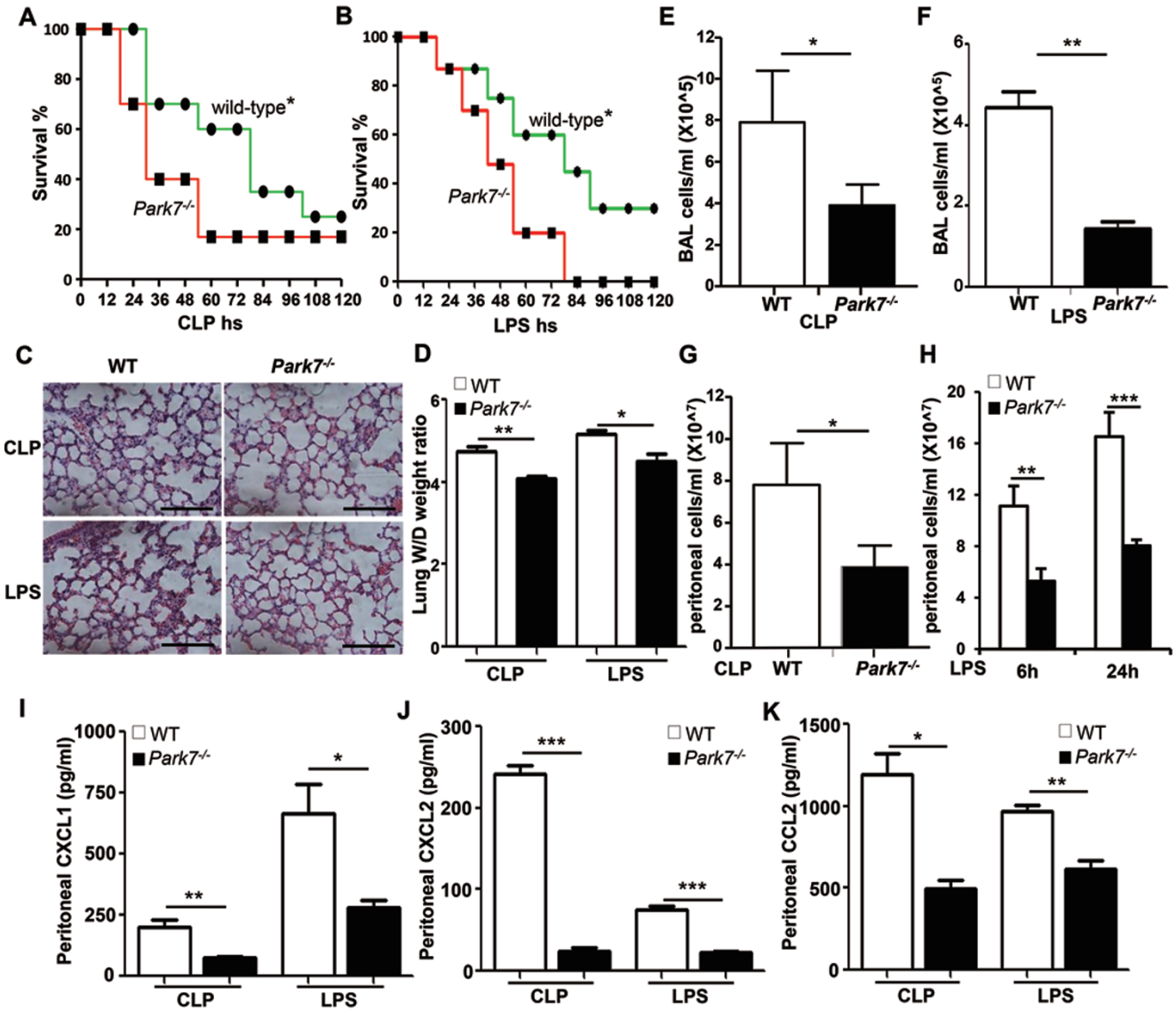

Figure 1 *Park7*$^{-/-}$ mice were more sensitive to CLP- and LPS-induced septic shock. **(A, B)** Survival of WT and *Park7*$^{-/-}$ mice subjected to CLP (n = 20/group) **(A)** and LPS (n = 10/group) **(B)**. Data were analyzed using log-rank test. *P < 0.05. **(C)** Representative sections of HE staining for lung infiltration of inflammatory cells 24 h after CLP and LPS (n = 5/group). Magnification, 40×. **(D)** Lung wet/dry ratio 24 h after CLP and LPS. **(E, F)** Quantification of inflammatory cells in collected BAL fluid 24 h after CLP **(E)** and LPS treatment **(F)**. **(G)** Quantification of inflammatory cells in peritoneal lavage fluid 24 h after CLP (n = 5/group). **(H)** Quantification of inflammatory cells in peritoneal lavage fluid after LPS treatment at the indicated time points. **(I-K)** CXCL1 **(I)**, CXCL2 **(J)** and CCL2 **(K)** concentrations in peritoneal lavage fluid of WT and *Park7*$^{-/-}$ mice 24 h after CLP or LPS treatment (n = 5/group). Data were analyzed using Student's t-test. *P < 0.05; **P < 0.01; ***P < 0.001.

show that, in sepsis models, the significantly attenuated production of IL-6 and TNF-α in *Park7*$^{-/-}$ mice is IL-10-independent and is at least partially because of the impaired cytokine production in *Park7*$^{-/-}$ macrophages after endotoxin treatment.

Toll-like receptor signaling was blunted in Park7-deficient macrophages

Toll-like receptors (TLRs) recognize pathogen-derived macromolecules, and play an important role in macrophage activation [21, 22]. As Park7 deficiency impaired macrophage cytokine production, we then examined the role of Park7 in TLR signaling. Compared with WT, *Park7*$^{-/-}$ peritoneal macrophages produced less IL-6 and

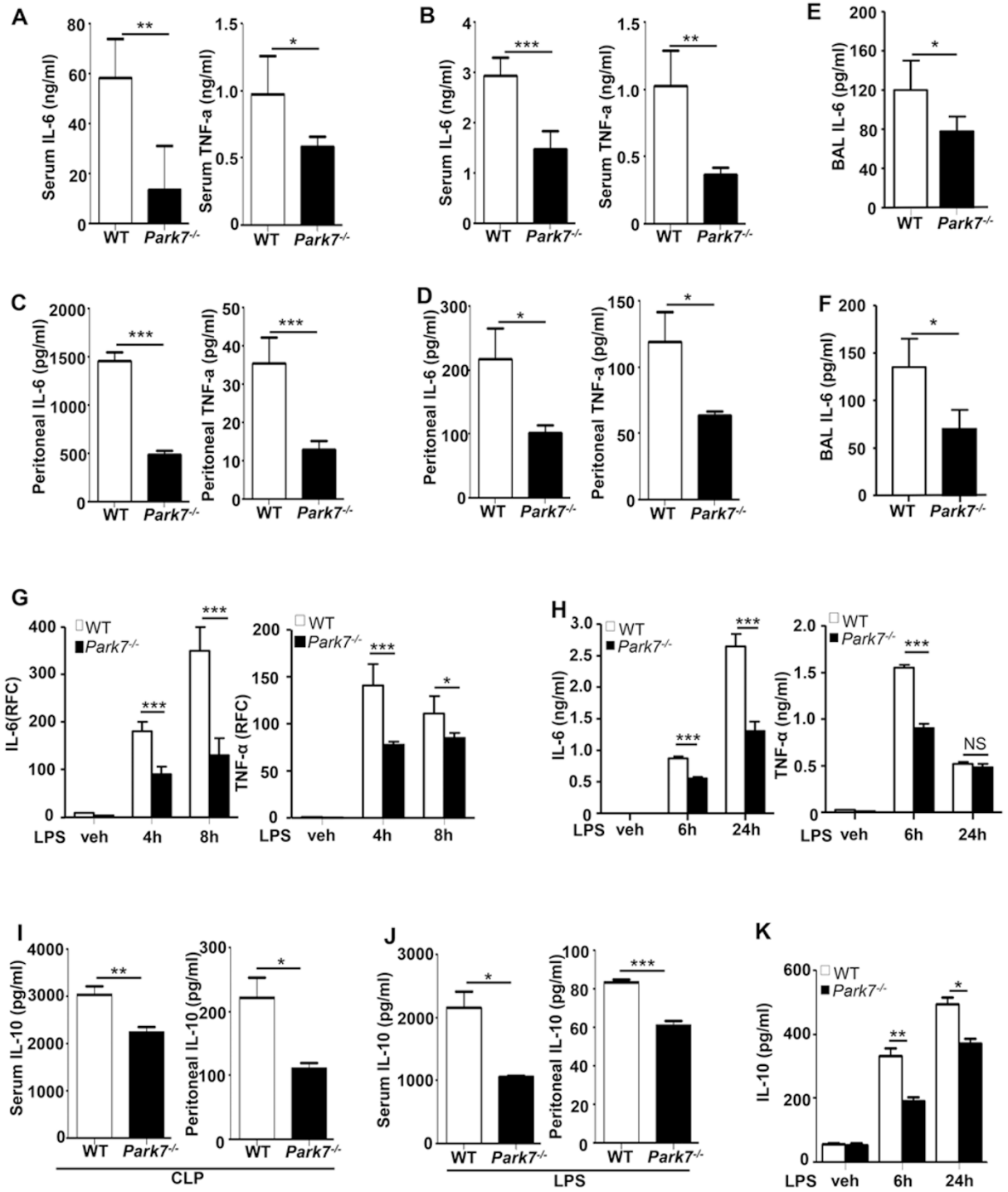

Figure 2 Disruption of *Park7* reduces proinflammatory cytokine induction during CLP- and LPS-induced septic shock. **(A**, **B)** IL-6 and TNF-α serum concentrations of WT and *Park7*$^{-/-}$ mice 24 h after CLP **(A)** or LPS treatment **(B)** (*n* = 5/group). **(C**, **D)** IL-6 and TNF-α levels in peritoneal lavage fluid of WT and *Park7*$^{-/-}$ mice 24 h after CLP **(C)** or LPS treatment **(D)** (*n* = 5/group). **(E**, **F)** IL-6 levels in BAL fluid of WT and *Park7*$^{-/-}$ mice 24 h after CLP **(E)** or LPS treatment **(F)** (*n* = 5/group). **(G**, **H)** Quantification of mRNA **(G)** and protein levels **(H)** of IL-6 and TNF-α, at the indicated time points, in peritoneal macrophages after LPS treatment . **(I**, **J)** IL-10 concentrations in serum or peritoneal lavage fluid 24 h after CLP **(I)** or LPS treatment **(J)**. **(K)** Quantification of IL-10 protein levels, at the indicated time points, in peritoneal macrophages after LPS treatment. Data were analyzed using Student's *t*-test. **P* < 0.05; ***P* < 0.01; ****P* < 0.001. RFC, relative fold change.

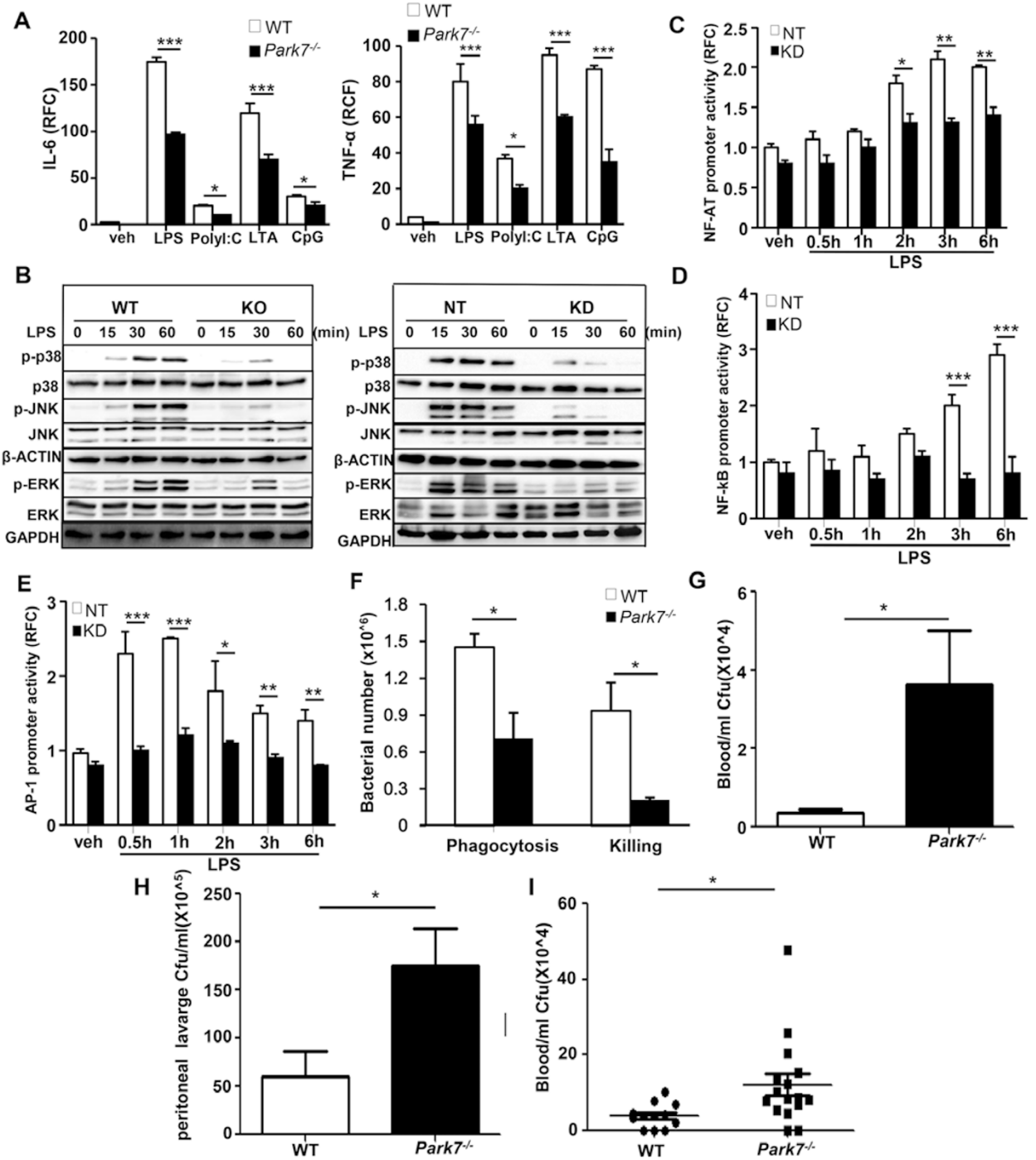

Figure 3 *Park7* depletion affects macrophage activation after LPS treatment. **(A)** Quantification of mRNA expression of IL-6 and TNF-α in macrophages upon treatment with various pathogen-derived macromolecules, including LPS (100 ng/ml), Poly I:C (20 μg/ml), LTA (10 μg/ml) and CpG.(1 μM; *n* = 4/group). **(B)** Phosphorylated p38, JNK and ERK shown by immunoblotting in WT and *Park7*$^{-/-}$ primary macrophages or NT and KD, at the indicated time points, upon LPS. **(C-E)** Transcriptional activities of NF-AT **(C)**, NF-κB **(D)** and AP-1 **(E)** by luciferase reporter assay in NT and KD, at the indicated time points, after LPS treatment. **(F)** Phagocytosis and killing of bacteria by peritoneal macrophages isolated from WT and *Park7*$^{-/-}$ mice (*n* = 3/group). **(G, H)** Quantification of bacterial burden in blood **(G)** and peritoneal lavage fluid **(H)** 24 h after CLP (*n* = 3/group). **(I)** Quantification of bacterial burden in blood of mice facing imminent death after a lethal dose of LPS challenge. Data were analyzed using Student's *t*-test. **P* < 0.05; ***P* < 0.01; ****P* < 0.001.

TNF-α after LPS, PolyI:C, LTA or CpG ODN treatment (Figure 3A). Next, we assessed the activation of MAPKs, NF-κB and TBK-IRF3 signaling pathways downstream of TLRs in primary macrophages and RAW264.7 [23]. Thirty min after LPS stimulation, activation of MAPKs was significantly lower in KO and KD macrophages than that in WT and NT, respectively (Figure 3B). In addition, phosphorylation of IκB-α and IRF3 was remarkably decreased in KD compared with NT (Supplementary information, Figure S3). Because AP-1, NF-AT and NF-κB are known transcription factors downstream of MAPKs and NF-κB pathways [24-26], we examined their transactivation by luciferase reporter assays. Compared with NT, KD had markedly decreased luciferase activity after LPS treatment (Figure 3C-3E). Given that TLR signaling augments macrophage bactericidal activity [8], we assessed the bactericidal activity in peritoneal macrophages of WT and *Park7*$^{-/-}$ 1 h after incubation with *E. coli*. Impaired phagocytosis and bacterial killing abilities were observed in *Park7*$^{-/-}$ macrophages compared with WT ones (Figure 3F). Consequently, the bacterial burdens in blood or peritoneal lavage fluid were greater in *Park7*$^{-/-}$ mice compared with WT mice 24 h after CLP (Figure 3G and 3H).

We then determined whether the increased bacterial burden also contributes to the higher mortality of *Park7*$^{-/-}$ mice after LPS treatment. We employed a novel strategy to detect bacterial burdens in mice facing imminent death after a lethal LPS challenge. Body temperature of mice was monitored every 6 h in the first 24 h and hereafter every 12 h after LPS. We artificially defined the mice with body temperature below 32 degrees as dying ones [27], and sacrificed them for bacterial burden measurement. At the end of this experiment (5 days), 12 out of 20 WT mice and 16 out of 20 KO mice were sacrificed. No bacteria were detected in peritoneal fluid (data not shown). However, significantly higher bacterial burden was observed in blood of *Park7*$^{-/-}$ mice compared with WT mice (Figure 3I). These results show that *Park7* deficiency severely blunts the TLR signaling and consequently impairs the bactericidal ability of macrophages, and strongly suggest that the higher mortality of *Park7*$^{-/-}$ mice from sepsis is caused by increased bacteria burden.

Park7 deficiency impairs NADPH oxidase-dependent ROS production in macrophages

As ROS produced by NADPH oxidase have an established role in regulating TLR signaling [12, 28], we assessed whether Park7 could modulate the accumulation of NADPH oxidase-derived ROS. Intracellular ROS were quantified through dichlorofluorescin diacetate staining followed by flow cytometry or lucigenin-derived chemilumiscence in RAW264.7 and peritoneal macrophages. After 4 h LPS treatment, greatly reduced induction of intracellular ROS was observed in *Park7*$^{-/-}$ and KD macrophages compared with WT and NT ones, respectively (Figure 4A and 4B). The decline of ROS in *Park7*-deficient macrophages apparently did not result from increase of ROS scavengers, because the expression of *Nfe2l2* and its downstream targets, *Gclm* and *Trx1* [29-31], was either comparable between *Park7*$^{-/-}$ and WT macrophages or decreased in *Park7*$^{-/-}$ macrophages compared with WT ones (Supplementary information, Figure S4). To specifically target NADPH oxidase, we adopted phorbol-12-myristate-13-acetate (PMA) to exclusively stimulate for NOX-dependent respiratory burst. PMA caused dramatic ROS induction in WT and NT macrophages but not in *Park7*-deficient ones (Figure 4C-4F). Given that the main ROS produced by NADPH oxidase is superoxide anion, we adopted another assessment to measure the superoxide by combining a widely used sensitive superoxide ($O_2^{\cdot-}$) probe, Dihydroethidium (DHE), with HPLC method. Because DHE oxidation yields two fluorescent products, 2-hydroxyethidium (EOH) and ethidium, and EOH is known to be more specific for $O_2^{\cdot-}$ than ethidium, we used HPLC analysis to measure EOH levels to assess $O_2^{\cdot-}$ production or NADPH oxidase activity [32]. As shown in Figure 4G, under the PMA treatment, WT macrophages generated more superoxide anion than *Park7*$^{-/-}$ macrophages.

Restoration of Park7 expression rescues ROS production and inflammatory responses in Park7$^{-/-}$ *macrophages*

To test the specificity of Park7 on NADPH oxidase-dependent ROS production, we assessed whether re-expression of *Park7* can rescue the ROS production by NADPH oxidase. Stable transfectants with doxycycline-induced *Park7* expression were established in NT and KD and named NT-Park7 and KD-Park7, respectively. Doxycycline-induced *Park7* expression was detected by qPCR and immunoblotting (Figure 5A and 5B). ROS production was restored in doxycycline-treated KD-Park7 after PMA stimulation (Figure 5C). In response to ROS restoration, IL-6 and TNF-α production was also reinstated (Figure 5D and 5E). Similar restoration of IL-6 and TNF-α production was detected in KD-Park7 cells treated with LPS (Figure 5F and 5G). These results indicate that restoration of Park7 expression rescues NADPH oxidase-dependent ROS production and in turn reinstates the production of proinflammatory cytokines.

ROS modulate LPS-induced proinflammatory cytokine production in macrophages

As, upon LPS stimulation, the induction of ROS and

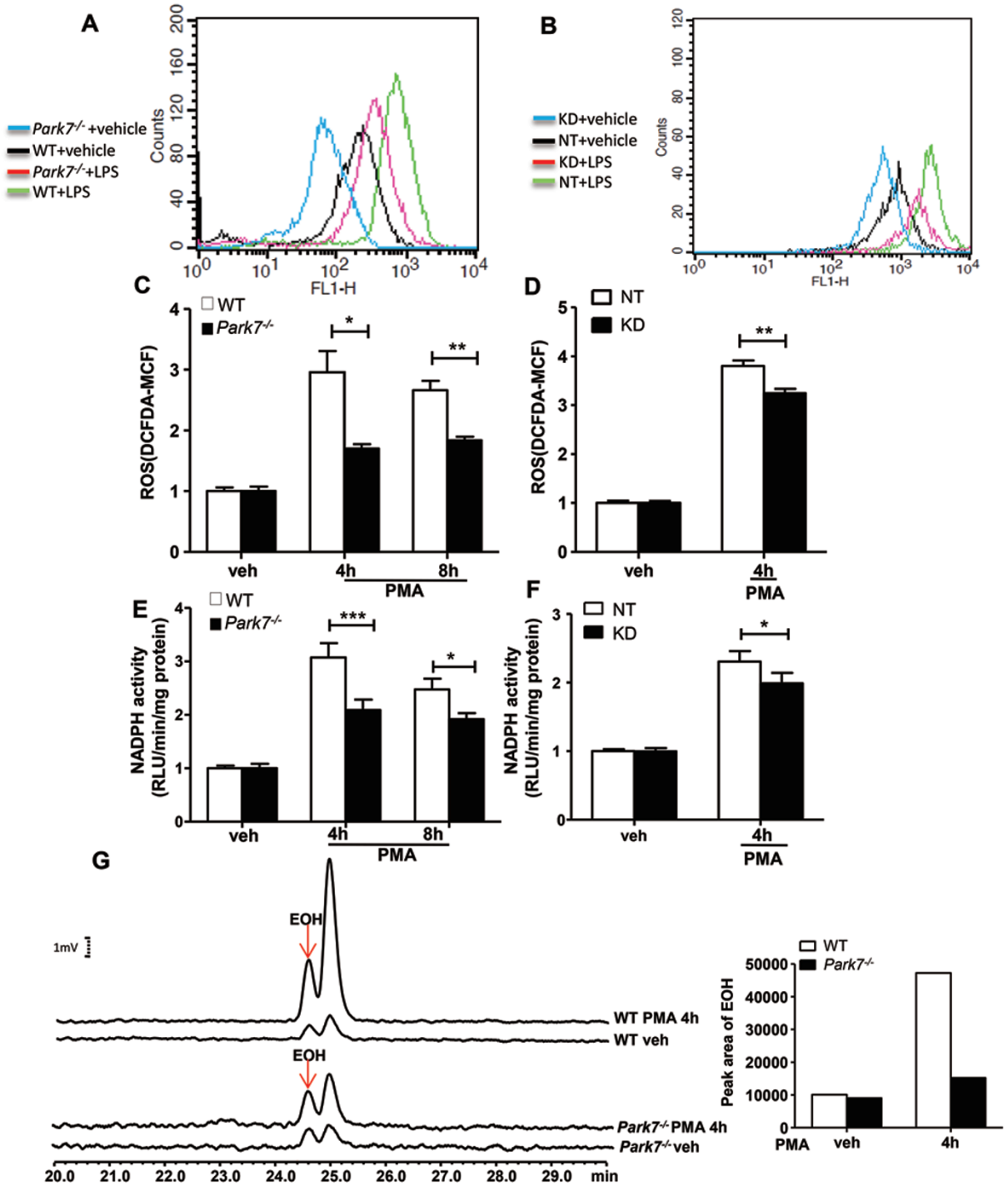

Figure 4 Depletion of *Park7* results in impaired LPS- and PMA-induced ROS production in macrophages. **(A**, **B)** Quantification of cellular ROS levels by oxidized DCFDA and flow cytometry in peritoneal macrophages isolated from WT and *Park7*$^{-/-}$ mice **(A)** or in NT and KD RAW264.7 cells **(B)** 4 h after LPS. **(C**, **D)** Quantification of ROS, at the indicated time points, by DCFDA staining in WT and *Park7*$^{-/-}$ macrophages **(C)** or in NT and KD RAW264.7 cells **(D)** after PMA stimulation. **(E**, **F)** Quantification of superoxide, at the indicated time points, by lucigenin-derived chemiluminescence in WT and *Park7*$^{-/-}$ macrophages **(E)** or in NT and KD RAW264.7 cells **(F)**. **(G)** HPLC analysis of DHE-derived products in WT and *Park7*$^{-/-}$ peritoneal macrophages after PMA (100 ng/ml) stimulation for 4 h. Data were analyzed using Student's *t*-test. **P* < 0.05; ***P* < 0.01; ****P* < 0.001.

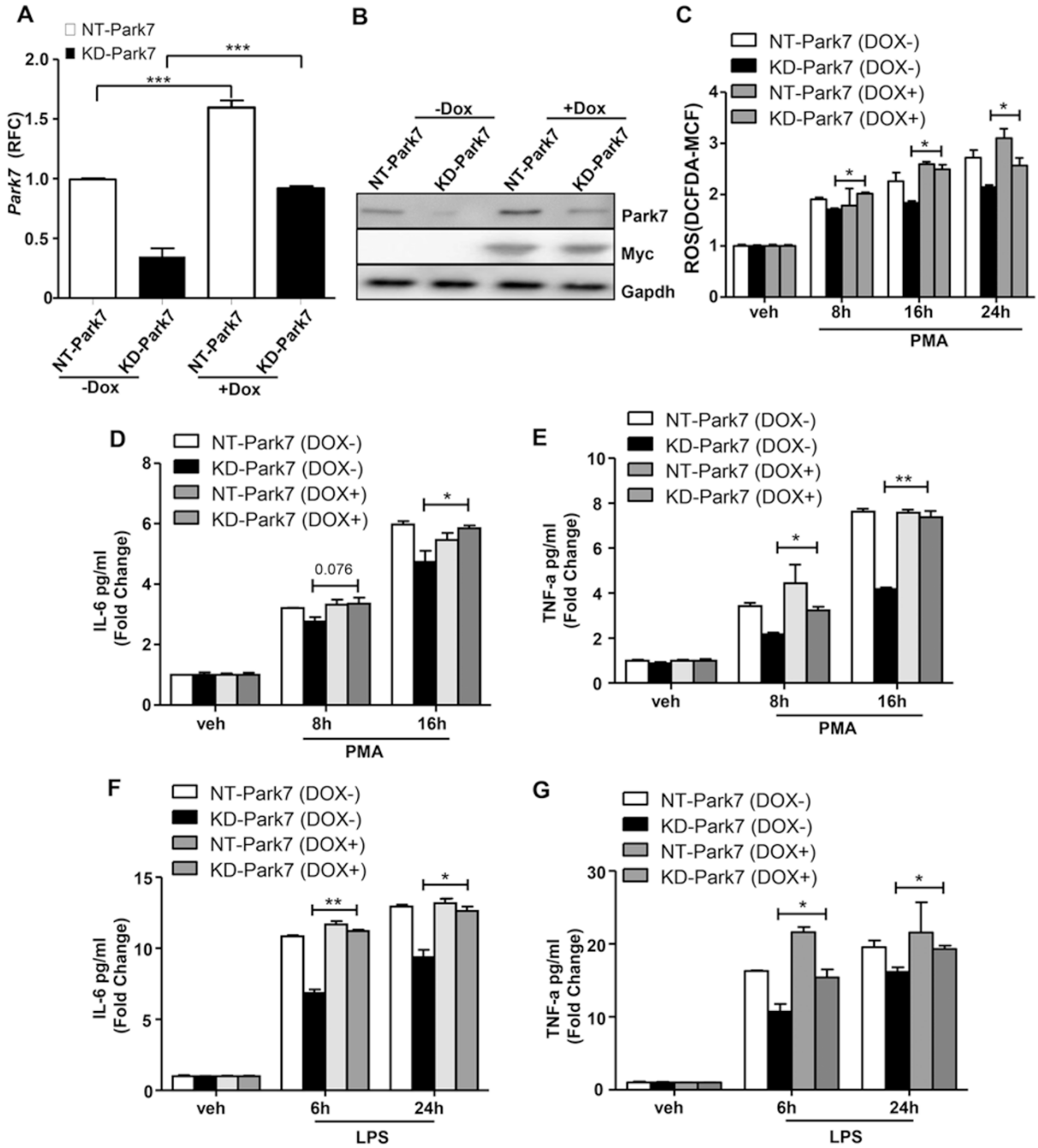

Figure 5 Restored expression of *Park7* rescues the ROS and proinflammatory cytokine production in *Park7*-deficient macrophages. **(A**, **B)** Quantification of *Park7* mRNA and protein levels by qPCR **(A)** and western blotting **(B)**, respectively, in NT-Park7 and KD-Park7 RAW264.7 cells after doxycycline (1 μg/ml) treatment. **(C)** ROS levels, at the indicated time points, by DCFDA staining after PMA stimulation. **(D**, **E)** IL-6 **(D)** and TNF-α **(E)**, at the indicated time points, in culture media by ELISA after PMA treatment. **(F**, **G)** IL-6 **(F)** and TNF-α **(G)**, at the indicated time points, in culture media by ELISA after LPS treatment. Data were analyzed using Student's *t*-test. **P* < 0.05; ***P* < 0.01; ****P* < 0.001.

proinflammatory cytokines was decreased in *Park7*$^{-/-}$ macrophages, we investigated whether administration of an exogenous oxidant could augment proinflammatory cascade. IL-6 and TNF-α levels were measured in *Park7*$^{-/-}$ macrophages 6 h after treatment with LPS (1 ng) or LPS along with H_2O_2 (10 μM). Exposure of H_2O_2

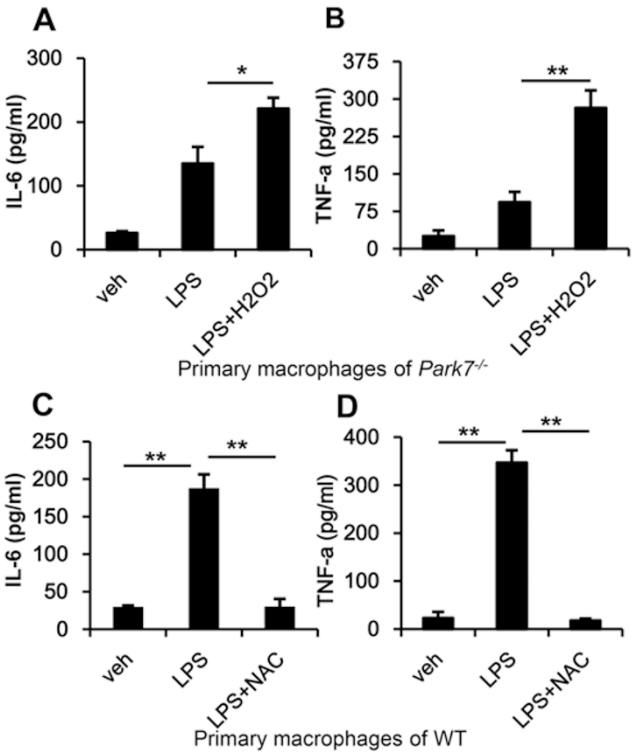

Figure 6 ROS enhance LPS-induced proinflammatory cytokine production in macrophages. **(A**, **B)** IL-6 **(A)** and TNF-α **(B)** levels by ELISA in *Pakr7*$^{-/-}$ macrophages 6 h after H_2O_2 (10 μM) and LPS (1 ng/ml) treatment. **(C**, **D)** IL-6 **(C)** and TNF-α **(D)** levels by ELISA in WT macrophages 6 h after NAC (0.5 mM) and LPS (10 ng/ml) treatment. Data were analyzed using Student's *t*-test. **P* < 0.05; ***P* < 0.01; ****P* < 0.001.

significantly increased the levels of LPS-induced IL-6 and TNF-α expression in *Park7*$^{-/-}$ macrophages (Figure 6A and 6B). To answer whether ROS elimination could inhibit proinflammatory cascade, we treated WT macrophages with LPS (10 ng) or LPS along with antioxidant NAC (0.5 mM). After 6-h treatment, NAC significantly reduced IL-6 and TNF-α levels (Figure 6C and 6D). These results indicate that ROS play a critical role in modulating proinflammatory cytokine production in macrophages.

Park7 interacts with p47^{phox} *to activate NADPH oxidase*

NADPH oxidase is composed of six subunits including gp91^{phox}, p22^{phox}, p40^{phox}, p67^{phox}, p47^{phox} and rac2. Given that the function of Park7 is partially mediated by physical interactions with other proteins like TP53 [33] and PTEN [34], we then examined putative interactions between Park7 and the NADPH oxidase subunits. We employed DOMINE to search for putative domains binding to Park7 [35, 36]. This search identified several putative interacting domains including catalase, DJ-1/PfpI family, PX domain and so on. Interestingly, both p47^{phox} and p40^{phox} contain PX domains, suggesting their putative interactions with Park7. Immunoprecipitation indicated no interaction between Park7 and p40^{phox} (data not shown). Interaction of endogenous Park7 and p47^{phox} was observed in NT as well as in KD but with a much decreased level (Figure 7A). Remarkably, this interaction was enhanced in NT after LPS challenge in a time-dependent manner (Figure 7A). As Cys106 oxidation is important for Park7 interaction with other proteins [37], we then examined whether Park7 was oxidized in our experimental system. NT cells showed significantly increased Park7 oxidation after PMA treatment (Supplementary information, Figure S8), suggesting that the enhanced Park7-p47^{phox} interaction may be attributed to the increased Park7 oxidation level. Given that phosphorylation and plasma membrane translocation of p47^{phox} are key events for NADPH oxidase assembly [38], we investigated whether Park7 is required for activation of NADPH oxidase via modulating p47^{phox} phosphorylation and membrane translocation. LPS and PMA treatment induced significant p47^{phox} phosphorylation and membrane accumulation in NT but not in KD, respectively (Figure 7A and 7B). In agreement, fluorescent staining demonstrated membrane translocation of p47^{phox} in NT but not in KD upon PMA stimulation (Figure 7C). Given that Rac2 plays a critical role in the assembly and activation of NADPH oxidase [39], we then investigated whether Rac2 could affect the Park7-p47^{phox} interaction. Immunoprecipitation indicated that Rac2 knockdown had no effect on this interaction (Supplementary information, Figure S5). Taken together, these results suggest that, by interacting with p47^{phox} and modulating phosphorylation and membrane translocation of p47^{phox}, Park7 affects NADPH oxidase activation.

The C-terminus of Park7 is required for the physical association with p47^{phox}

To characterize the functional region(s) of Park7 contributing to p47^{phox} interaction, we constructed a series of doxycycline-inducible Myc-tagged expression vectors encoding truncated Park7 (Figure 8A). ND, CD and MD stand for N-terminal, C-terminal and middle-domain deletion, respectively. Inducible expression of truncated Park7 in stable transfectants was detected by immunoblotting (Supplementary information, Figure S6). CD80 was undetectable. Immunoprecipitation indicated that Park7-CD40 was not able to interact with p47^{phox} (Figure 8B), suggesting that the C-terminus of Park7 is indispensible for this interaction. Like full-length Park7, en-

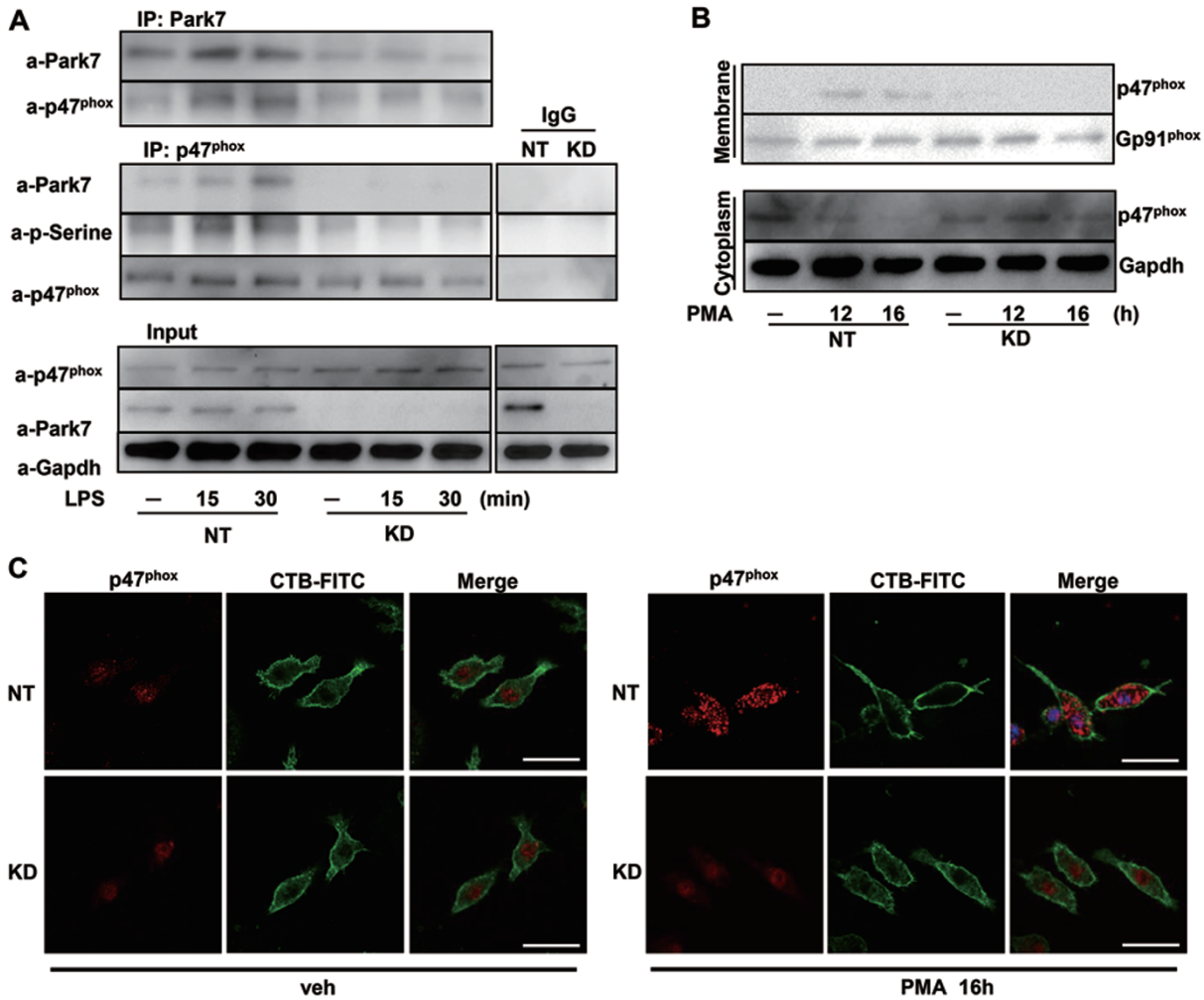

Figure 7 Park7 interacts with p47^{phox} to activate NADPH oxidase. **(A)** Interaction between endogenous p47^{phox} and Park7, at the indicated time points, in both NT and KD RAW264.7 cells by immunoprecipitation and western blotting after LPS. **(B)** p47^{phox} levels in both membrane and cytoplasm fractions, at the indicated time points, in both NT and KD RAW264.7 cells by western blotting after LPS. **(C)** Fluorescent staining of p47^{phox} and membrane of NT and KD RAW264.7 cells 16 h after PMA stimulation. CTB-FITC, Cholera Toxin B Subunit-FITC. Magnification, 40×.

hanced interaction between truncated Park7 and p47^{phox} was also observed upon LPS treatment (Figure 8B). To answer whether this interaction is important for NADPH oxidase activation, we overexpressed ND40 and CD40 in *Park7*-deficient macrophages. ND40, but not CD40, rescued PMA-induced ROS production by NADPH oxidase (Figure 8C). In response to this ROS change, LPS-induced IL-6 and TNF-α production was also rescued by ND40 but not CD40 (Figure 8D and 8E). These data suggest that the C-terminus of Park7 is required for Park7-p47^{phox} interaction which is critical for NADPH oxidase activation and proinflammatory cytokine production in macrophages.

Macrophages with restored Park7 expression confer strong protection against severe sepsis

To assess the therapeutic potential of Park7 on sepsis, we adopted a RAW264.7-based macrophage reconstituted mouse model, which was successfully used to reconstitute macrophage-depleted allogeneic BALB/c mice [40]. Given BALB/c origin of RAW264.7 cells, we first examined whether RAW264.7 cells will be eliminated by immune repelling in B6 host mice. We used a fluorescent vital dye SP-DiI (D-7777, Molecular Probes) to stain the RAW264.7 cells, and then transferred these labeled RAW264.7 cells into C57BL/6 or BALB/C mice with or without $GdCl_3$ pretreatment. 24 h or 3 days after transferring, the mice were sacrificed and the lungs, livers

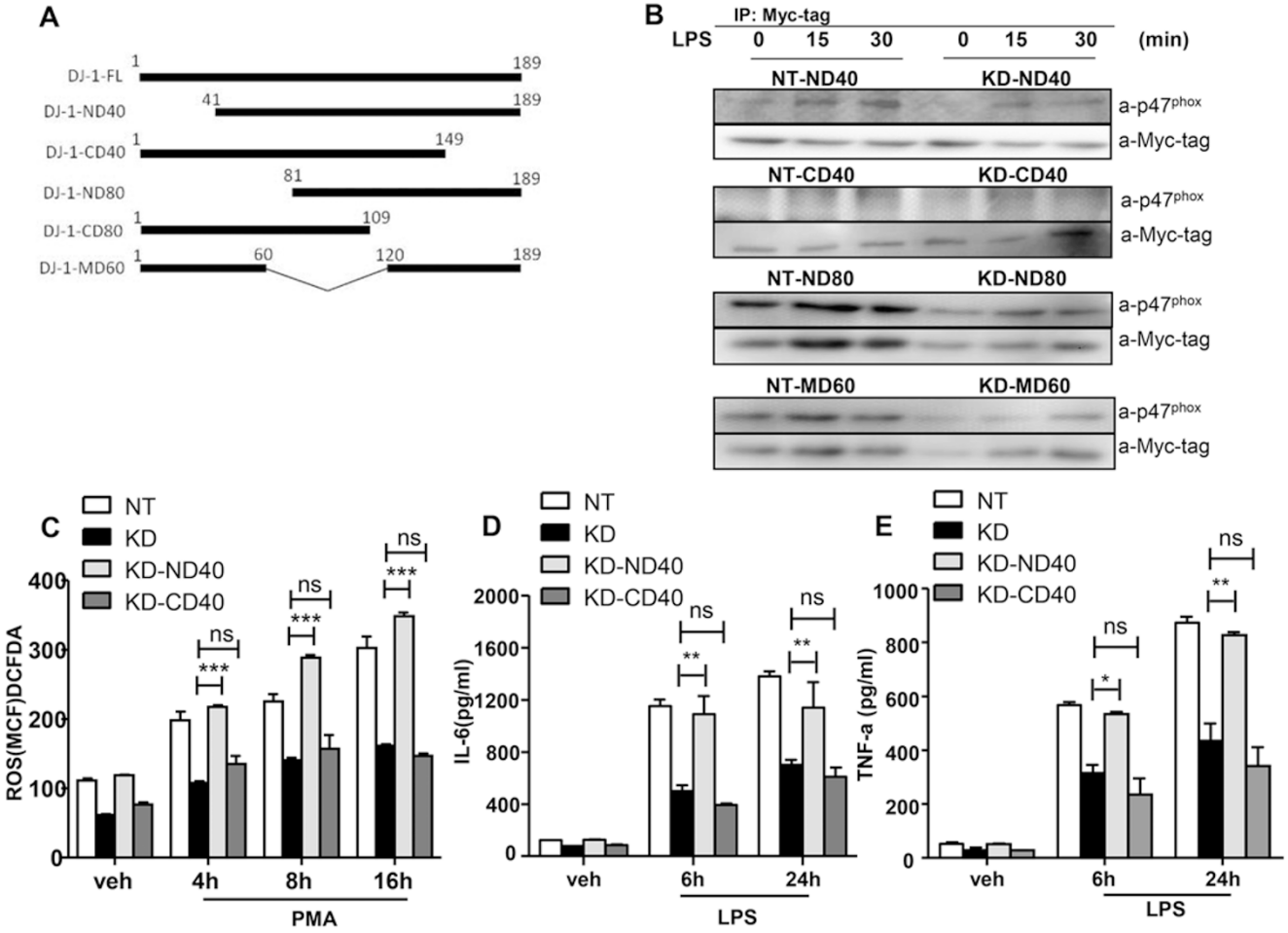

Figure 8 Characterization of the interaction between p47^{phox} and Park7. **(A)** Diagram of five truncated Park7 fragments cloned into a doxycycline-inducible expression vector followed by a Myc-tag. **(B)** Interactions between p47^{phox} and truncated Park7, at the indicated time points, by immunoprecipitation and western blotting after LPS. **(C)** NADPH oxidase-dependent ROS production, at the indicated time points, in RAW264.7 cells with ND40 and CD40 expression after PMA stimulation. **(D**, **E)** IL-6 **(D)** and TNF-α **(E)** levels by ELISA, at the indicated time points, in RAW264.7 cells with ND40 and CD40 expression after LPS treatment. Data were analyzed using Student's *t*-test. **P* < 0.05; ***P* < 0.01; ****P* < 0.001.

and spleens were collected. The fluorescent signals were examined under fluorescent microscope. In the group without $GdCl_3$ pretreatment, compared with BALB/c mice, great immune repelling was observed in B6 mice with RAW264.7 transferring (Supplementary information, Figure S7A and S7B). However, in the $GdCl_3$-treated group, the intensity and pattern of fluorescent signals on RAW264.7 cells were comparable in both allogeneic and syngeneic transplantation. These results clearly demonstrated that RAW264.7 cells were not eliminated by either immune repelling or $GdCl_3$-mediated killing in macrophage-depleted C57BL/6 mice in at least 3 days (Supplementary information, Figure S7A and S7B). Then, KD-Park7 RAW264.7 cells were treated with or without doxycycline and injected i.v. into mice depleted of macrophages (Figure 9A). Lethal dose of LPS treatment was carried out 24 h after transferring. Survival was monitored every 12 h. 90% of mice with KD-Park7 (−Dox) transferring died while only 50% of mice transferred with KD-Park7 (+Dox) died by the end of the experiment, whereas mice transferred with NT pretreated with or without doxycycline showed no survival difference (Figure 9B). In response to the improved survival rate, significantly decreased bacterial burden was detected in the blood of mice transferred with KD-Park7 (+Dox) compared with the ones with KD-Park7 (−Dox) transferring (Figure 9C). In addition, elevated IL-6 and TNF-α levels in both serum and peritoneal lavage and increased

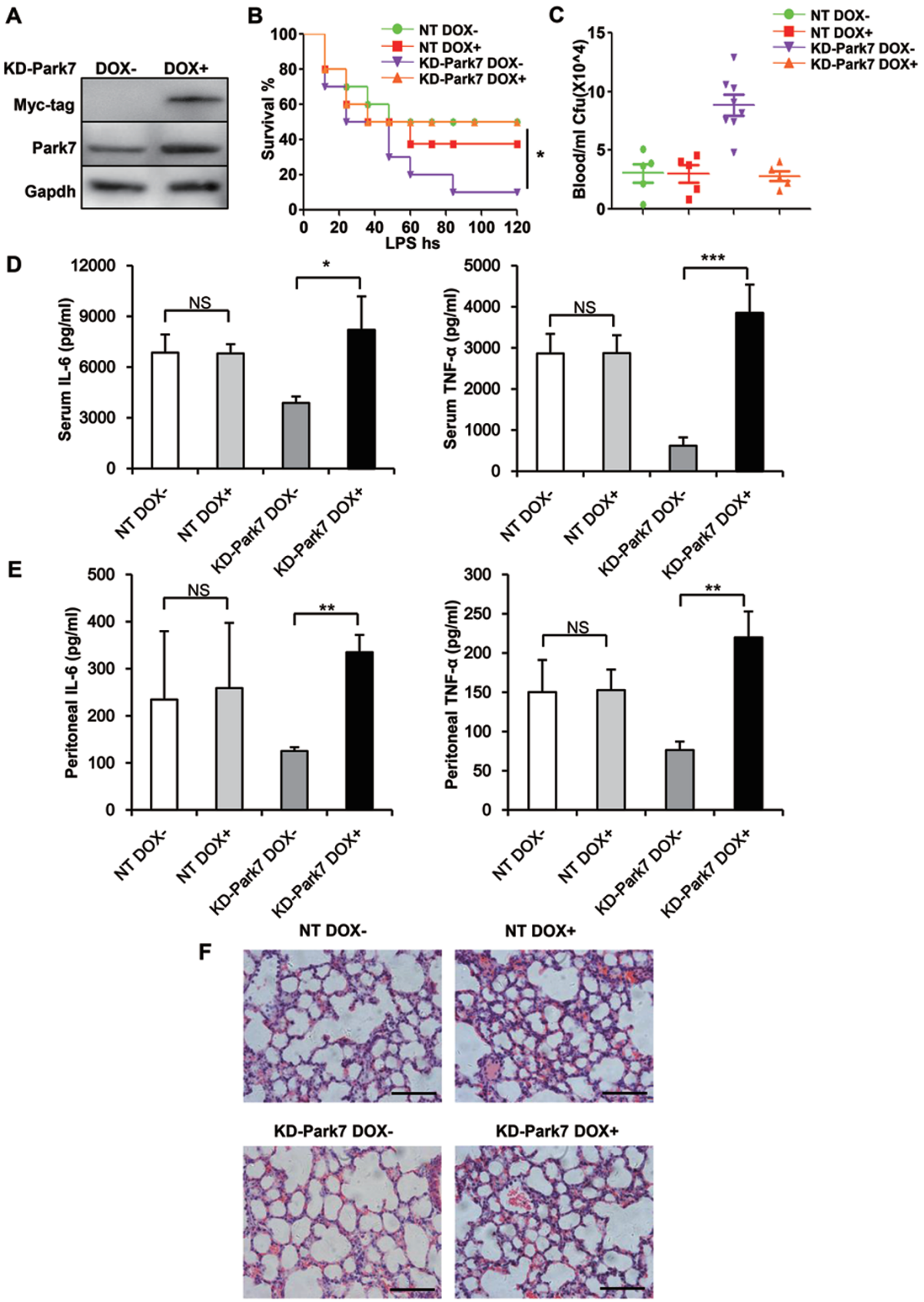
A
KD-Park7
DOX-
DOX+
Myc-tag
Park7
Gapdh
B
NT DOX-
NT DOX+
KD-Park7 DOX-
KD-Park7 DOX+
Survival %
LPS hs
*
C
NT DOX-
NT DOX+
KD-Park7 DOX-
KD-Park7 DOX+
Blood/ml Cfu(X10^4)
D
Serum IL-6 (pg/ml)
NS
*
Serum TNF-α (pg/ml)
NS
***
NT DOX-
NT DOX+
KD-Park7 DOX-
KD-Park7 DOX+
E
Peritoneal IL-6 (pg/ml)
NS
**
Peritoneal TNF-α (pg/ml)
NS
**
NT DOX-
NT DOX+
KD-Park7 DOX-
KD-Park7 DOX+
F
NT DOX-
NT DOX+
KD-Park7 DOX-
KD-Park7 DOX+

lung infiltration of inflammatory cells were also observed in mice transferred with KD-Park7 (+Dox) 24 h after a nonlethal dose of LPS challenge (Figure 9D-9F). These results strongly suggest that forced Park7 expression acts as a putative therapeutic option against septic shock.

Discussion

We have shown that *Park7*$^{-/-}$ mice have greater susceptibility to CLP- and LPS-induced sepsis, which is associated with impaired bactericidal ability of macrophages in *Park7*$^{-/-}$ mice. Furthermore, we demonstrate that forced expression of Park7 restored macrophage activation characterized by recovered production of ROS and proinflammatory cytokines in *Park7*$^{-/-}$ macrophages. More importantly, mice transferred with Park7-restored macrophages showed significantly improved survival along with decreased bacterial burdens and reinforced proinflammatory responses in LPS-induced sepsis. Through its C-terminus, Park7 could interact with p47^{phox} and facilitate its phosphorylation and membrane translocation, which in turn result in the NADPH oxidase activation.

LPS-induced septic death is largely dependent on excessive inflammatory response. Compared with WT mice, however, we demonstrated that *Park7*$^{-/-}$ mice are more susceptible to LPS-induced sepsis accompanied by impaired cytokine and chemokine production. Interestingly, similar phenomenon was also observed by Foster's group in *Stat2*$^{-/-}$ mice [41]. These findings strongly suggest the existence of an alternative, cytokine storm-independent mechanism of LPS-induced septic death. In fact, we demonstrated that the significant bacteremia may contribute to the higher susceptibility of *Park7*$^{-/-}$ mice to LPS-induced septic death.

In p53-null but not in p53 WT MEF cells, Vasseur *et al*. [42] have recently demonstrated that *Park7* knockdown could lead to reduced ROS accumulation. However, we showed that Park7 is essential for ROS induction upon LPS treatment in p53 WT macrophages. This discrepancy could be explained by Hassan's [43] observation that LPS inhibits p53 activation in macrophages. Therefore, these results indicate that Park7 could direct ROS induction in p53-null or -inactive cells. Given 57% of sepsis patients infected with gram-negative bacteria, Park7 could have broad therapeutic potential for sepsis. On the other side, as inactivation or mutation of p53 are frequent in tumors, whether Park7 controls ROS production in tumors will be an intriguing question to answer.

As far as we know, we for the first time demonstrate that Park7 is involved in ROS production in a NADPH oxidase-dependent manner. This function of Park7 relies on its C-terminal interaction with p47^{phox}. Upon LPS challenge, we observed an enhanced interaction between Park7 and p47^{phox} concomitant with elevated phosphorylation and membrane translocation of p47^{phox}. Similar to the *Park7*$^{-/-}$ mice, leukocytes from *p47*^{phox} knockout mice also showed impaired capabilities to produce superoxide and kill staphylococci [44]. The exact mechanism responsible for the enhancement of the Park7-p47^{phox} interaction after LPS remains to be determined. However, recent studies demonstrated that both p47^{phox} and Park7 could be recruited into lipid rafts under the stimulation of LPS [45, 46], suggesting that the enhanced interaction between Park7 and p47^{phox} may be due to their sub-cellular spatial changes.

ROS are not only cytotoxic molecules, but also signaling molecules regulating a wide variety of physiological processes. For example, by regulating TLRs-initiated signaling pathways, ROS appear to modulate the production of proinflammatory cytokines [11, 47]. In the present study, addition of H_2O_2 enhanced LPS-induced proinflammatory cytokine production in *Park7*$^{-/-}$ macrophages, whereas NAC reduced proinflammatory cytokine levels in WT macrophages. These results further confirm the strong link between ROS and proinflammatory cytokines.

An uncontrolled release of proinflammatory cytokines, thought to lead to multiple organ failure and even death, is an important characteristic in early stage of sepsis [48, 49]. Many agents with anti-inflammatory potency were tested for sepsis therapy but with limited or no success [50]. Most recently, accumulating evidence indicates that sepsis has a late immunosuppression stage characterized by lymphopenia and loss of immune function [4], and this stage seems responsible for the majority of death of

Figure 9 *Park7* restoration strongly protects against LPS-induced sepsis. **(A)** Doxycycline-induced Park7 expression detected by western blotting. **(B)** Survival of macrophage-depleted mice after transferring with NT (Dox−), NT (Dox+), KD-Park7 (Dox−) or KD-Park7 (Dox+) macrophages followed by LPS challenge (n = 10/group). Data were analyzed using log-rank test. *P < 0.05. **(C)** Quantification of bacterial burden in blood of dying mice subjected to macrophage transferring followed by a lethal dose of LPS challenge. **(D**, **E)** IL-6 and TNF-α levels in serum **(D)** and peritoneal lavage fluid **(E)** of mice subjected to macrophage transferring 24 h after LPS (n = 5/group). **(F)** Representative sections of HE staining for lung infiltration of inflammatory cells of mice subjected to macrophage transferring 24 h after LPS (n = 5/group). Magnification, 40×. Data were analyzed using Student's t-test. *P < 0.05; **P < 0.01; ***P < 0.001.

septic patients [5, 6]. In our sepsis models, *Park7*$^{-/-}$ mice present immunosuppression phenotypes similar to the late stage of sepsis, suggesting that *Park7*$^{-/-}$ mice could serve as an ideal animal model for studying the immunopathophysiology of the late stage of sepsis. Actually, we demonstrate that restoration of Park7 expression in macrophages could improve survival in LPS-induced sepsis. This provides a possibility that agents that can induce *Park7* expression may have clinical value to treat sepsis in late stage.

Materials and Methods

Mouse strains

Mice were bred and maintained under SPF conditions. *Park7*$^{-/-}$ mice (stock#: 006577) were purchased from The Jackson Laboratory (Bar Harbor, Maine, USA). Littermate controls of matched age and sex were used in all experiments.

Measurement of bacterial burden in mice facing imminent death after LPS

Mice (20/group) were i.p. injected with LPS (15 mg/kg BW) and the rectal temperature was measured every 6 h in the first 24 h and hereafter every 12 h after LPS injection. Mice with temperature below 32 °C were artificially defined as dying ones and sacrificed for collection of blood and peritoneal lavage. 10 μl blood or peritoneal fluid was immediately diluted in 990 μl PBS and 100 μl of the dilution was plated onto Agar-plate for 24 h incubation at 37 °C. Results were presented as CFU/ml.

Cell stimulation and extraction of HPLC

WT and *Park7*$^{-/-}$ peritoneal macrophages were grown in six-well plates at 3 × 10^6 cells/well in 1640 medium supplemented with 10% fetal bovine serum. Cells were starved for 1 h before stimulation with PMA (100 ng/ml) for 4 h. After stimulation, cells were washed twice with cold PBS and incubated in PBS/DTPA (500 μl) at final DHE concentration of 50 μM for additional 30 min. After incubation, cells were washed twice with cold PBS, harvested in acetonitrile (500 μl/well), sonicated (10 s, 1 cycle at 8 W), and centrifuged at 12 000× g for 10 min at 4 °C. Supernatants were dried under vacuum and pellets were stored at −20 °C in the dark until analysis. Samples were resuspended in 120 μl PBS/DTPA and 100 μl was injected into HPLC system.

HPLC conditions of analysis

The conditions of HPLC experiment were as described previously [32]. The optimal emission wavelength for both EOH and ethidium detection is 595 nm. Chromatographic separation was carried out with the use of a NovaPark C18 column (4.6 × 250 mm, 5 μm particle size) in a HPLC system equipped with a rheodyne injector and ultraviolet detector (SPD-M20A) and fluorescence detectors (RF-10A). Solutions A (pure acetonitrile) and B (water/10% acetonitrile/0.1% trifluoroacetic acid) were used as a mobile phase at a flow rate of 0.4 ml/min. Runs were started with 0% solution A, increased linearly to 40% solution A during the initial 10 min, kept at the proportion of 100% solution A for additional 5 min, and to 0% solution A for the final 10 min. DHE was monitored by ultraviolet absorption at 245 nm. EOH and ethidium were monitored by fluorescence detection with excitation at 510 nm and emission at 595 nm. Quantification was performed by comparison of integrated peak areas between the WT and *Park7*$^{-/-}$ cell supernatants under identical chromatographic conditions.

Standard solution: 100 μm DHE was incubated with xanthine/xanthine oxidase (0.5 mM/0.05 U/ml) in PBS buffer composed of (in mM) 7.78 Na_2HPO_4, 2.20 KH_2PO_4, 140 NaCl and 2.73 KCl, pH 7.4, containing 100 μM DTPA at 37 °C for 30 min. EOH was separated by HPLC, collected and lyophilized to dryness. The purple-pink solid was further resuspended in DMSO and used as standard.

Adoptive transfer of macrophages

Macrophage transferring was performed according to a published method with slight modification [40]. Briefly, C57BL/6 mice were injected i.v. with $GdCl_3$ (Sigma-Aldrich) to eliminate macrophages. 24 h after $GdCl_3$ injection, KD-Park7 macrophages (1 × 10^6) were injected i.v. into mice. Another 24 h later, mice were injected i.p. with LPS. Survival was monitored for 5 days.

Statistical analysis

Except survival studies, all other results were presented as mean ± SEM from at least 3 independent biologically replicated experiments. Data were analysed using Student's *t*-test. $*P < 0.05$; $**P < 0.01$; $***P < 0.001$.

Acknowledgments

We thank Dr Liwei Dong (The Second Military Medical University) for the luciferase reporter vectors, Dr Li Shen (Tongji University School of Medicine) for the *Pseudomonas aeruginosa* and Dr Dechun Feng (National Institute on Alcohol Abuse and Alcoholism) for helpful comments. This work was supported by the Ministry of Science and Technology of China (2012CB966800 and 2013CB945600) to WQG, the National Natural Science Foundation of China (81130038 and 81372189 to WQG, and 31300742 to XK), the Science and Technology Commission of Shanghai Municipality (Pujiang program), the Shanghai Health Bureau Key Disciplines and Specialties Foundation, the Shanghai Education Committee Key Discipline and Specialties Foundation (J50208) and KC Wong foundation and funds to WQG, and the Shanghai Education Committee (Eastern Scholar Program) to XK.

References

1 Hotchkiss RS, Opal S. Immunotherapy for sepsis — a new approach against an ancient foe. *N Engl J Med* 2010; **363**:87-89.
2 Angus DC, van der Poll T. Severe sepsis and septic shock. *N Engl J Med* 2013; **369**:840-851.
3 Huber-Lang M, Barratt-Due A, Pischke SE, *et al*. Double blockade of CD14 and complement C5 abolishes the cytokine storm and improves morbidity and survival in polymicrobial sepsis in mice. *J Immunol* 2014; **192**:5324-5331.
4 Boomer JS, To K, Chang KC, *et al*. Immunosuppression in patients who die of sepsis and multiple organ failure. *JAMA* 2011; **306**:2594-2605.
5 Meisel C, Schefold JC, Pschowski R, *et al*. Granulocyte-macrophage colony-stimulating factor to reverse sepsis-associated

immunosuppression: a double-blind, randomized, placebo-controlled multicenter trial. *Am J Respir Crit Care Med* 2009; **180**:640-648.
6 Schefold JC, Hasper D, Volk HD, Reinke P. Sepsis: time has come to focus on the later stages. *Med hypotheses* 2008; **71**:203-208.
7 Kanayama A, Miyamoto Y. Apoptosis triggered by phagocytosis-related oxidative stress through FLIPS down-regulation and JNK activation. *J Leukoc Biol* 2007; **82**:1344-1352.
8 West AP, Brodsky IE, Rahner C, *et al*. TLR signalling augments macrophage bactericidal activity through mitochondrial ROS. *Nature* 2011; **472**:476-480.
9 McCubrey JA, Lahair MM, Franklin RA. Reactive oxygen species-induced activation of the MAP kinase signaling pathways. *Antioxid Redox Signal* 2006; **8**:1775-1789.
10 Takada Y, Mukhopadhyay A, Kundu GC, Mahabeleshwar GH, Singh S, Aggarwal BB. Hydrogen peroxide activates NF-kappa B through tyrosine phosphorylation of I kappa B alpha and serine phosphorylation of p65: evidence for the involvement of I kappa B alpha kinase and Syk protein-tyrosine kinase. *J Biol Chem* 2003; **278**:24233-24241.
11 Bulua AC, Simon A, Maddipati R, *et al*. Mitochondrial reactive oxygen species promote production of proinflammatory cytokines and are elevated in TNFR1-associated periodic syndrome (TRAPS). *J Exp Med* 2011; **208**:519-533.
12 Kong X, Thimmulappa R, Kombairaju P, Biswal S. NADPH oxidase-dependent reactive oxygen species mediate amplified TLR4 signaling and sepsis-induced mortality in Nrf2-deficient mice. *J Immunol* 2010; **185**:569-577.
13 Hong Z, Shi M, Chung KA, *et al*. DJ-1 and alpha-synuclein in human cerebrospinal fluid as biomarkers of Parkinson's disease. *Brain* 2010; **133**:713-726.
14 Yokota T, Sugawara K, Ito K, Takahashi R, Ariga H, Mizusawa H. Down regulation of DJ-1 enhances cell death by oxidative stress, ER stress, and proteasome inhibition. *Biochem Biophy Res Commun* 2003; **312**:1342-1348.
15 Martinat C, Shendelman S, Jonason A, *et al*. Sensitivity to oxidative stress in DJ-1-deficient dopamine neurons: an ES-derived cell model of primary Parkinsonism. *PLoS Biol* 2004; **2**:e327.
16 Kong X, Thimmulappa R, Craciun F, *et al*. Enhancing Nrf2 pathway by disruption of Keap1 in myeloid leukocytes protects against sepsis. *Am J Respir Crit Care Med* 2011; **184**:928-938.
17 Calandra T, Baumgartner JD, Grau GE, *et al*. Prognostic values of tumor necrosis factor/cachectin,interleukin-1, interferon-alpha, and interferon-gamma in the serum of patients with septic shock. Swiss-Dutch J5 Immunoglobulin Study Group. *J Infect Dis* 1990; **161**:982-987.
18 Damas P, Ledoux D, Nys M, Vrindts Y, De Groote D, Franchimont P, Lamy M. Cytokine serum level during severe sepsis in human IL-6 as a marker of severity. *Ann Surg* 1992; **215**:356-362.
19 Underhill DM, Ozinsky A. Phagocytosis of microbes: complexity in action. *Annu Rev Immunol* 2002; **20**:825-852.
20 Meador BM, Krzyszton CP, Johnson RW, Huey KA. Effects of IL-10 and age on IL-6, IL-1beta, and TNF-alpha responses in mouse skeletal and cardiac muscle to an acute inflammatory insult. *J Appl Physiol (1985)* 2008; **104**:991-997.
21 Lee CC, Avalos AM, Ploegh HL. Accessory molecules for Toll-like receptors and their function. *Nat Rev Immunol* 2012; **12**:168-179.
22 Gallego C, Golenbock D, Gomez MA, Saravia NG. Toll-like receptors participate in macrophage activation and intracellular control of Leishmania (Viannia) panamensis. *Infect Immun* 2011; **79**:2871-2879.
23 Akira S, Takeda K. Toll-like receptor signaling. *Nat Rev Immunol* 2004; **4**:499-511.
24 Karin M. The regulation of AP-1 activity by mitogen-activated protein kinases. *J Biol Chem* 1995; **270**:16483-16486.
25 Pahl HL. Activators and target genes of Rel/NF-kappaB transcription factors. *Oncogene* 1999; **18**:6853-6866.
26 Wu CC, Hsu SC, Shih HM, Lai MZ. Nuclear factor of activated T cells c is a target of p38 mitogen-activated protein kinase in T cells. *Mol Cell Biol* 2003; **23**:6442-6454.
27 Warn PA, Brampton MW, Sharp A, *et al*. Infrared body temperature measurement of mice as an early predictor of death in experimental fungal infections. *Lab Anim* 2003; **37**:126-131.
28 Nakahira K, Kim HP, Geng XH, *et al*. Carbon monoxide differentially inhibits TLR signaling pathways by regulating ROS-induced trafficking of TLRs to lipid rafts. *J Exp Med* 2006; **203**:2377-2389.
29 Kensler TW, Wakabayashi N, Biswal S. Cell survival responses to environmental stresses via the Keap1-Nrf2-ARE pathway. *Annu Rev Pharmacol Toxicol* 2007; **47**:89-116.
30 Foller M, Harris IS, Elia A, *et al*. Functional significance of glutamate-cysteine ligase modifier for erythrocyte survival in vitro and in vivo. *Cell Death Differ* 2013; **20**:1350-1358.
31 Im JY, Lee KW, Woo JM, Junn E, Mouradian MM. DJ-1 induces thioredoxin 1 expression through the Nrf2 pathway. *Hum Mol Genet* 2012; **21**:3013-3024.
32 Fernandes DC, Wosniak J, Pescatore LA, *et al*. Analysis of DHE-derived oxidation products by HPLC in the assessment of superoxide production and NADPH oxidase activity in vascular systems. *Am J Physiol Cell Physiol* 2007; **292**:C413-C422.
33 Kato I, Maita H, Takahashi-Niki K, *et al*. Oxidized DJ-1 inhibits p53 by sequestering p53 from promoters in a DNA-binding affinity-dependent manner. *Mol Cell Biol* 2013; **33**:340-359.
34 Kim YC, Kitaura H, Taira T, Iguchi-Ariga SM, Ariga H. Oxidation of DJ-1-dependent cell transformation through direct binding of DJ-1 to PTEN. *Int J Oncol* 2009; **35**:1331-1341.
35 Yellaboina S, Tasneem A, Zaykin DV, Raghavachari B, Jothi R. DOMINE: a comprehensive collection of known and predicted domain-domain interactions. *Nucleic Acids Res* 2011; **39**:D730-D735.
36 Raghavachari B, Tasneem A, Przytycka TM, Jothi R. DOMINE: a database of protein domain interactions. *Nucleic Acids Res* 2008; **36**:D656-D661.
37 Waak J, Weber SS, Gorner K, *et al*. Oxidizable residues mediating protein stability and cytoprotective interaction of DJ-1 with apoptosis signal-regulating kinase 1. *J Biol Chem* 2009; **284**:14245-14257.
38 Lambeth JD. NOX enzymes and the biology of reactive oxygen. *Nat Rev Immunol* 2004; **4**:181-189.
39 Anderson KE, Chessa TA, Davidson K, *et al*. PtdIns3P and

Rac direct the assembly of the NADPH oxidase on a novel, pre-phagosomal compartment during FcR-mediated phagocytosis in primary mouse neutrophils. *Blood* 2010; **116**:4978-4989.

40 Kong XN, Yan HX, Chen L, *et al*. LPS-induced down-regulation of signal regulatory protein {alpha} contributes to innate immune activation in macrophages. *J Exp Med* 2007; **204**:2719-2731.

41 Alazawi W, Heath H, Waters JA, *et al*. Stat2 loss leads to cytokine-independent, cell-mediated lethality in LPS-induced sepsis. *Proc Natl Acad Sci USA* 2013; **110**:8656-8661.

42 Vasseur S, Afzal S, Tomasini R, *et al*. Consequences of DJ-1 upregulation following p53 loss and cell transformation. *Oncogene* 2012; **31**:664-670.

43 Hassan F, Islam S, Mu MM, *et al*. Lipopolysaccharide prevents doxorubicin-induced apoptosis in RAW 264.7 macrophage cells by inhibiting p53 activation. *Mol Cancer Res* 2005; **3**:373-379.

44 Jackson SH, Gallin JI, Holland SM. The p47phox mouse knock-out model of chronic granulomatous disease. *J Exp Med* 1995; **182**:751-758.

45 Kim K S, Kim J S, Park J Y, *et al.* DJ-1 associates with lipid rafts by palmitoylation and regulates lipid rafts-dependent endocytosis in astrocytes. *Hum Mol Genet*, 2013. **22**:4805-4817.

46 Choi Y K, Elaine D, Kwon Y G, *et al*. Regulation of ROS production and vascular function by carbon monoxide. *Oxid Med Cell Longev* 2012; **2012**:794237.

47 Rada B, Gardina P, Myers TG, Leto TL. Reactive oxygen species mediate inflammatory cytokine release and EGFR-dependent mucin secretion in airway epithelial cells exposed to Pseudomonas pyocyanin. *Mucosal immunol* 2011; **4**:158-171.

48 Annane D, Bellissant E, Cavaillon JM. Septic shock. *Lancet* 2005; **365**:63-78.

49 Spooner CE, Markowitz NP, Saravolatz LD. The role of tumor necrosis factor in sepsis. *Clin Immunol Immunopathol* 1992; **62**:S11-S17.

50 Suffredini AF, Munford RS. Novel therapies for septic shock over the past 4 decades. *JAMA* 2011; **306**:194-199.

(**Supplementary information** is linked to the online version of the paper on the *Cell Research* website.)